Editorial Manager(tm) for Bulletin of Earthquake Engineering
Manuscript Draft

Manuscript Number:

Title: Frequency variation in site response over long and short time scales, as observed from strong motion data of the L'Aquila (2009) seismic sequence

Article Type: SI: 2010 L'Aquila Earthquake

Keywords: strong motion; subsoil non-linearity; Horizontal to Vertical Spectral Ratio; Standard Spectral Ratio; 1D modeling; S-Transform

Corresponding Author: Puglia Rodolfo

Corresponding Author's Institution:

First Author: Puglia Rodolfo

Order of Authors: Puglia Rodolfo;Rocco Ditommaso;Francesca Pacor;Marco Mucciarelli;Lucia Luzi;Marcello Bianca

Manuscript
Click here to download Manuscript: site_resp_freq_variation_from_strong_motion_data_of_L_Aquila_2009_sequence.doc Click here to view linked References

BULLETIN OF EARTHQUAKE ENGINEERING
Special Issue: "The L'Aquila earthquake? A view of site effects and structural behavior from temporary networks"
Guest editors: M. Mucciarelli, S. Parolai, G. Cultrera

Submitted: December, 2010

Title: Frequency variation in site response over long and short time scales, as observed from strong motion data of the L'Aquila (2009) seismic sequence

Authors: R. Puglia* (1), R. Ditommaso (2), F. Pacor (1), M. Mucciarelli (2), L. Luzi (1), M. Bianca (2)

(1) Istituto Nazionale di Geofisica e Vulcanologia, Milano, Italy
(2) Di.S.G.G., Basilicata University, Potenza, Italy

Contact details (corresponding author)*:
Dr. Rodolfo Puglia
Istituto Nazionale di Geofisica e Vulcanologia
Sezione di Milano-Pavia
via Bassini 15
20133 Milano, Italy
ph.: (+39) 02 23699259
fax: (+39) 02 23699267
email: rodolfo.puglia@mi.ingv.it

Frequency variation in site response over long and short time scales, as observed from strong motion data of the L'Aquila (2009) seismic sequence

R. Puglia[1], R. Ditommaso[2], F. Pacor[1], M. Mucciarelli[2], L. Luzi[1], M. Bianca[2]

1) Istituto Nazionale di Geofisica e Vulcanologia, Milano, Italy

2) Di.S.G.G., Basilicata University, Potenza, Italy

Abstract Previous works based mainly on strong-motion recordings of large Japanese earthquakes showed that site amplification and soil fundamental frequency could vary over long and short time scales. These phenomena were attributed to non-linear soil behaviour due to inelastic, softening non-linearity: the starting fundamental frequency and amplification were both decreasing and not recovering for a time varying from few hours to several months. The recent April 6th 2009 earthquake (M_W 6.3), occurred in the L'Aquila district (central Italy), gave us the possibility to test hypotheses on time variation of amplification function and soil fundamental frequency, thanks to the recordings provided by a pre-existing strong-motion array and by a large number of temporary stations. We performed spectral ratio studies for the permanent stations of the Aterno Valley array where a reference station was available. The temporary stations and permanent ones were studied using time-frequency analyses through the S-Transform approach (Stockwell *et al*., 1996). Finally, analyses on noise recordings were performed, in order to study the soil behaviour in linear conditions. The results provided puzzling evidences. Concerning the long time scale, little variation was observed at the permanent stations of the Aterno Valley array. As for the short time-scale variation, the evidence was often contrasting, with some station showing a time-varying behavior, while others did not change their frequency with respect to the one evaluated from noise HVSR. Even when a time-varying fundamental frequency was observed, it was difficult to attribute it to a classical, softening non-linear behaviour. Even for the strongest recorded shocks, with PGA reaching 0.7 g, variations in frequency and amplitude seems not relevant from building design standpoint. The only exception seems to be the site named AQV, where the analyses evidence a fundamental frequency of the soil, shifting from 3 Hz to about 1.5 Hz during the mainshock.

Introduction

The variability of soil response has been observed on Japanese strong motion data by different authors on different data sets: Rubinstein *et al*. (2007) for the 2003 Tokachi-Oki earthquake, Sawazaki *et al*. (2009) for the 2000 Western-Tottori Earthquake, and Wu et al. (2009) for the 2004 Mid-Niigata earthquake. In all cases the main shock caused a reduction of fundamental soil frequency (up to 50%) and a subsequent recovery. All the authors agree on pointing out soil non-linear behavior as the cause for the observed variation, and observe different time intervals required for restoring the original soil frequency (from less than a hour to more than 4 years) and on the thickness of soil affected by shear modulus degradation.

The latter issue was investigated in detail by De Martin *et al*. (2010) using data collected from a borehole station during the 2005 Fukuoka prefecture Western offshore earthquake. They showed qualitative evidence of nonlinearity during the mainshock, but, when inverting along the stratigraphic column, they observed that out of the eleven layers considered, six did not show any degradation of shear modulus and two had a level of degradation lower than the one expected from laboratory data. For two layers there was agreement between theoretical and observed degradation and only one layer showed more degradation than expected.

Non-linearity appears to be a more subtle phenomenon than usually modeled by the practitioner, and literature also reports cases of hardening non linearity in non-cohesive, partially saturated soils (Bonilla *et al*., 2005).

The recent April 6th 2009 earthquake (M_W 6.3), occurred in the L'Aquila territory (central Italy), gave us the possibility to test several hypotheses on the long- and short-timescale variation of amplification function and soil fundamental frequency. The 2009 L'Aquila seismic sequence was recorded by a pre-existing strong-motion array and by a large number of temporary stations. The Aterno Valley Array, operated by the Italian civil protection, provided recordings of background seismicity since 2000, as well as the recordings of the foreshocks, the mainshock and the aftershocks of the 2009 seismic sequence. A description of the array and of the characteristics of the recordings can be found in Zambonelli *et al*. (2010), while a detailed description of the temporary network deployed by several European research institutions is provided by Bergamaschi *et al*. (this volume).

In this study we analyze the ground motion recorded at strong-motion stations of the Aterno array as well as at temporary stations (Working Group ITACA, http://itaca.mi.ingv.it). In particular, the analyzed stations are: AQA, AQG, AQK, AQM, AQV, of the RAN network, and MI01, MI02, MI03 and MI05 of the temporary array. In order to study the intra- and inter-event soil frequency variations, different kinds of analyses were performed including time-frequency analyses through the S-Transform approach (Stockwell *et al*., 1996), which allows investigating non-stationary signals, by the evaluation of the local spectrum in the time-frequency domain. Finally, analyses on noise recordings were also performed, in order to study the soil behavior in linear conditions.

Instrumental and geotechnical characteristics of the recording sites

The Aterno river valley array has been installed by the Italian civil protection, as part of the Italian strong motion network (RAN, Gorini *et al*., 2010) in the time span 2000-2005. It is composed of seven digital stations aligned along a direction transversal to the major axis of the Aterno valley and one station installed inside L'Aquila town. We examined 4 stations of the array (Figure 1): AQV (centre of the valley) AQA (left side of the valley), AQM (right side) and AQK (located on L'Aquila downtown), whose main characteristics are listed in Table 1.

Stations AQA and AQV have been installed on the recent alluvial deposits of the Aterno river (Holocene, Ol in Figure 1) made of gravels alternated to thin layers of finer deposits, that reach a depth of about 50m in correspondence of station AQV, and about 30 m at the station AQA. The station AQM is also installed on Holocene alluvial fan deposits, very close to the calcareous outcrops (Figure 1). To the south, in correspondence of L'Aquila downtown, station AQK has been deployed on cemented breccias, which have a thickness of about 40m, superimposed on marls. The calcareous bedrock is not reached by the borehole, which stops at 50 m.

The shear wave velocity of the subsoil, showed in Figure 2, has been measured through down-hole and cross-hole tests at AQA, AQV and AQK (Working Group ITACA, http://itaca.mi.ingv.it). The first site is characterized by a shallow soil layer (about 10 m) with low velocity (about 250 m/s), a first velocity increase at 10 m, up to 800 m/s, and a second increase at 20 m where velocities become larger than 900 m/s.

The second station, AQV, is characterized by a superficial layer of about 50 m, with an almost constant shear wave velocity of about 500 m/s, then velocity increases up to 1250 m/s, in correspondence of the calcareous bedrock. Finally, station AQK has a profile characterized by a velocity inversion: the cemented breccias, with shear wave velocities of about 700 m/s at 40 m, overlay a marly layer, with velocities of 640 m/s.

After the mainshock occurrence, a temporary network was installed by INGV consisting in 4 accelerometers (MI01, MI02, MI03, MI05, see Bergamaschi et al; this issue and Table 1 and Figure 1). These stations recorded the strongest aftershocks of the sequence and worked in continuous mode for about one month. Station MI01 has been deployed on a calcareous outcrop, in the NE edge of the valley, nearby the village of Pescomaggiore. MI02 has been deployed at Paganica on Holocene deposits of alluvial fan origin, whose depths are larger than 30m. Station MI03 has been installed in the vicinity of the Onna village, in the middle of the Aterno river valley, in correspondence of Holocene alluvial deposits. Finally, station MI05, inside the village of Sant'Eusanio Forconese, is installed on a terraced level (ACT) made of gravels, which is probably directly superimposed on the calcareous bedrock.

Two *in-situ* tests are available in the middle Aterno valley (Figure 2): a DH test close to the MI02 station (Paga3) and a microtremor array in the vicinity of MI03 (Onna). The first test indicates few meters characterized by low velocity and an almost constant velocity of 400-500 m/s down to 30 m, although the detail indicates very frequent velocity changes, probably related to the alluvial fan deposits, characterized by a high heterogeneity. At MI03 an average shear wave velocity of about 400 m/s is observed down to 40 m, probably relevant to the superficial alluvial layer.

Table 1. Accelerometric stations analyzed in this study and related information. The star on the EC8 class indicates that the soil class is assigned on the base of geological and geophysiscal data (GEO). Direct estimation methods are: CH = Cross-Hole; DH = Down-Hole; DISP = inversion of dispersion curve obtained from array microtremor measurements. Instrumental characteristics are: full scale (FS) and sampling frequency (Freq). Number of records with M >3.5 and M between 3.0 and 3.5 are reported together with the minimum and maximum epicentral distance (R_{MIN} R_{MAX}), peak ground acceleration (PGA) and velocity (PGV) for the four stations of the RAN.

Station Code	EC8 Class	Class Source	Sensor	FS (g)	Freq (Hz)	Digitizer	Installation start time	Installation end time	#of rec. M>3.0 (M>3.5)	R_{MIN} R_{MAX} [km]	PGA_{MIN} PGA_{MAX} [cm/s^2]	PGV_{MIN} PGV_{MAX} [cm/s]
AQV	B	CH	Episensor FBA-3	1	50	Kinemetrics Etna	1997/01/01		112 (38)	0.8 20.3	0.8 644.2	0.15 42.72
AQM	A*	GEO	Episensor FBA-3	1	200	Kinemetrics Makalu	1997/07/01	2009/09/11	102 (47)	1.6 20.2	2.8 332.0	0.06 8.01
AQA	B	DH	Episensor FBA-3	1	200	Kinemetrics Etna	2001/04/17		(38)	2.5 20.4	1.4 435.4	0.02 31.92
AQK	B	DH	Episensor BA-3	1	200	Kinemetrics Makalu	2005/12/02		(51)	0.8 23.0	2.3 355.5	0.05 35.80
MI01	A*	GEO	Episensor FBA-3	2	200	Reftek-130	2009/04/07	2009/04/27				
MI02	B	DH	Episensor FBA-3	2	200	Reftek-130	2009/04/07	2009/04/29				
MI03	B	DISP	Episensor FBA-3	2	200	Reftek-130	2009/04/07	2009/07/31				
MI05	B*	GEO	Episensor FBA-3	2	200	Reftek-130	2009/04/07	2009/04/28				

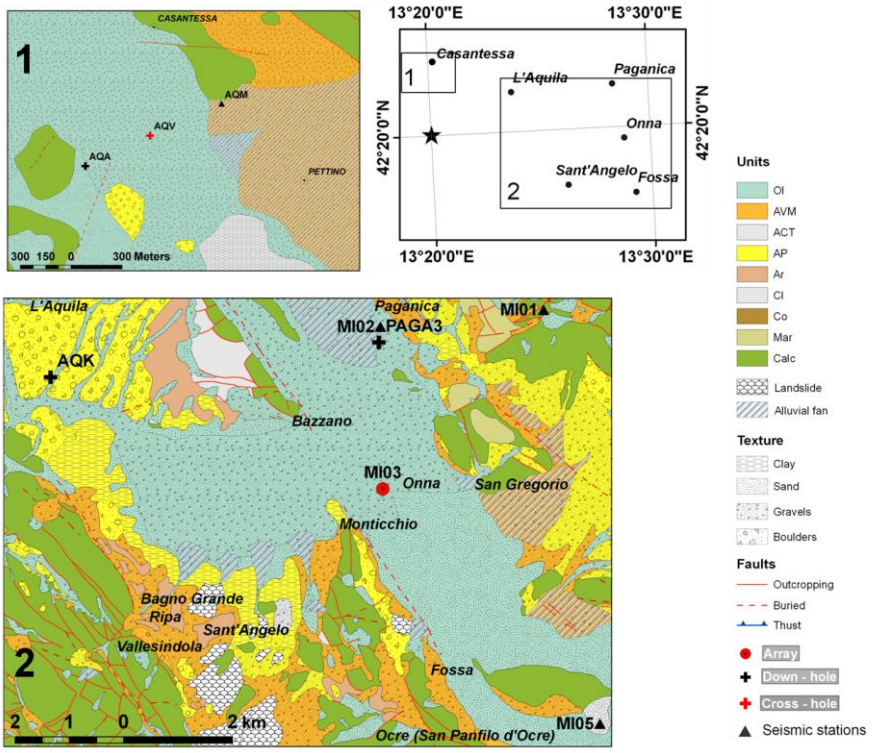

Fig. 1. Geological map and location of the analyzed stations. The insets in the upper right panel indicate the position of geological map of panel 1 and 2. Ol = Alluvial, lacustrine and swamp deposits, alluvial fan, eluvial-colluvial deposits (Holocene); AVM = *Sintema di valle Majelama*: deposits of alluvial, debris, glacial and landslide origin (upper Pleistocene); ACT = *Sintema di Catignano*: deposits of alluvial, debris, glacial and landslide origin (middle Pleistocene); AP = *Supersintema di Aielli - Pescina*: deposits of alluvial and debris origin alternated to lacustrine and swamp deposits (Pliocene - middle Pleistocene); Ar = Arenaceous-pelitic unit; Cl = Clay-marl unit; Calc = Limestones and marly limestones; Co = Conglomerates; Mar = Marls and marly limestones.

AQA ($V_{S,30}$ = 549 m/s)

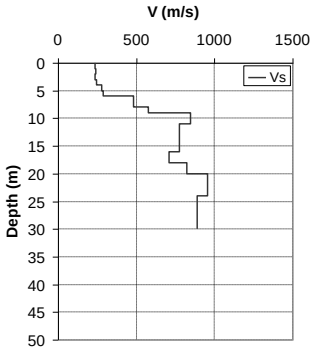

AQK ($V_{S,30}$ = 705 m/s)

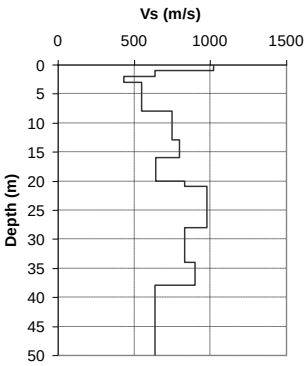

AQV ($V_{S,30}$ = 473 m/s)

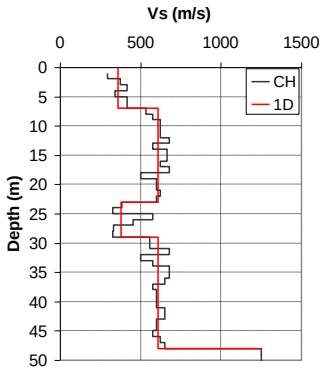

MI03 ($V_{S,30}$ = 378 m/s)

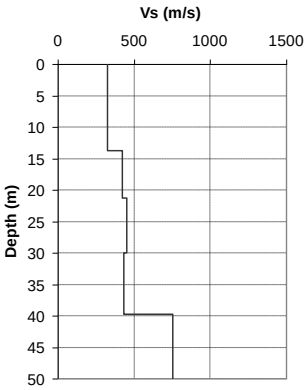

MI02 / Paga3 ($V_{S,30}$ = 379 m/s)

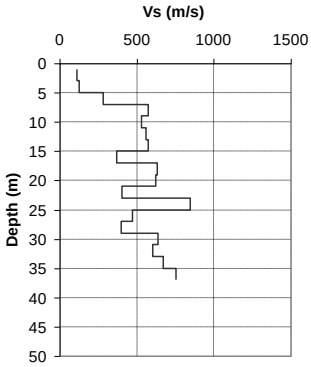

Fig. 2. Shear wave velocity profiles at 5 of the examined sites (for station AQV the simplified profile used in the 1D model is also reported).

Long time variation of site response

In this part of the work, the long time scale variation of the site fundamental frequency is investigated using strong-motion data recorded in the epicentral area. We focused our attention on the stations AQM, AQK, AQV and AQA (Figure 1), since good quality data are available before and during the sequence. In particular we selected waveforms recorded in 2009 from the 30th of March to the end of April, by the Aterno Valley array in the magnitude range 3.0-6.3. Unfortunately, during the L'Aquila mainshock, AQM station, set to 1g full-scale, saturated, due to a partial detachment of the instrument from the pillar; the recorded aftershocks have to be used carefully, although it can be reasonably supposed that no lifting of the box had occurred for seismic events of lower energy (Zambonelli *et al*., 2010). About 110 events were considered, with almost 45 earthquakes with magnitude larger than 3.5. Table 1 lists the number of records analyzed for each station. The waveforms were processed using the procedure proposed by Paolucci *et al*. (2009), which includes the baseline correction and band-pass filtering with a 2nd order a-causal frequency-domain Butterworth filter aimed to preserve the signal phase.

Spectral analysis

The first step of the analysis consisted in the extraction from the waveform of the S-wave phase and the signal coda. The former is a time window starting at the S wave arrival (t_{S1}), visually selected, and ending at time t_{S2}, evaluated on the base of the Arias intensity function (Arias, 1969) computed from the S-wave arrival (t_{S1}):

$$I(t) = \frac{\pi}{2g}\int_{t_{S1}}^{t} a^2(\tau)d\tau \qquad (1)$$

where $a(t)$ is the acceleration at time t and g is the gravity acceleration. The time t_{S2} is selected when the Arias intensity, normalized with respect to its maximum value, is 0.9. When the S-window includes surface waves, t_{S2} is manually reduced, in order to exclude these waves. It is found that generally the interval [t_{S1}, t_{S2}] is about 3.5s. We enlarged the windows relevant to AQK station to investigate frequencies down to 0.6 Hz, i.e. the fundamental frequency of this site (De Luca et al.; 2005, Bindi et al.; 2009). The coda window starts from twice after the S-wave travel time after the earthquake origin time (Herraiz and Espinosa , 1986) and ends after 10 s.

The S and coda windows were tapered along 5% of the window length using a cosine function and azimuthally projected on a ten-degree interval from 0 to 180. A

standard Fast Fourier Transform was then applied to the windows, padded with zeros to 2048 samples, which corresponds to about 10s of signal. The horizontal and vertical Fourier spectra were smoothed through the Konno and Ohmachi (1998) algorithm (with b = 40).

First the rotational Horizontal to Vertical Spectral Ratio (HVSR) and the Standard Spectral Ratio (SSR) were computed, using either the S wave window or the signal coda, for the events of magnitudes larger than 3.5. Figure 3 shows the mean HVSR curve for each azimuth. The curves obtained from the coda waves are generally similar to those calculated from the S-wave window, but with less scatter, consistently with the observation by Sawazaki *et al*. (2006), Mayeda *et al*. (2007) and Wu *et al*. (2009). The maximum discrepancy between the HVSR curves obtained with the two phases occurs at sites AQA and AQV. In particular, a stronger dependence on the direction is observed in the HVSRs obtained from the S phase, which leads to a high dispersion of the resonance amplitude and frequency.

Station AQM, installed at the border between the alluvial fan and calcareous bedrock (Figure 1), has a flat response in the frequency band 0.3-4 Hz with no preferential direction of the amplification. At higher frequencies, the HVSR amplitudes increase and vary with the direction, suggesting possible site amplification due to the presence of a thin alluvial layer over the bedrock. Therefore, this station can be used as a reference site in the SSR analysis for frequencies lower than 4 Hz. For this reason we do not consider station AQA in the SSR analysis since its fundamental frequency is very similar to that of AQM.

Figure 4 shows the horizontal rotational SSR curves, computed for stations AQK and AQV, using AQM as reference. An agreement between HVSR and SSR curves is observed for AQV at frequencies lower than 4 Hz for the different phases. Spectral ratios calculated from the coda waves are more stable for AQV than for AQK, as in the latter case, the coda is highly contaminated by the presence of surface waves and the vertical component of the motion is amplified at about 1 Hz (Figure 3 and Bindi et al. 2009).

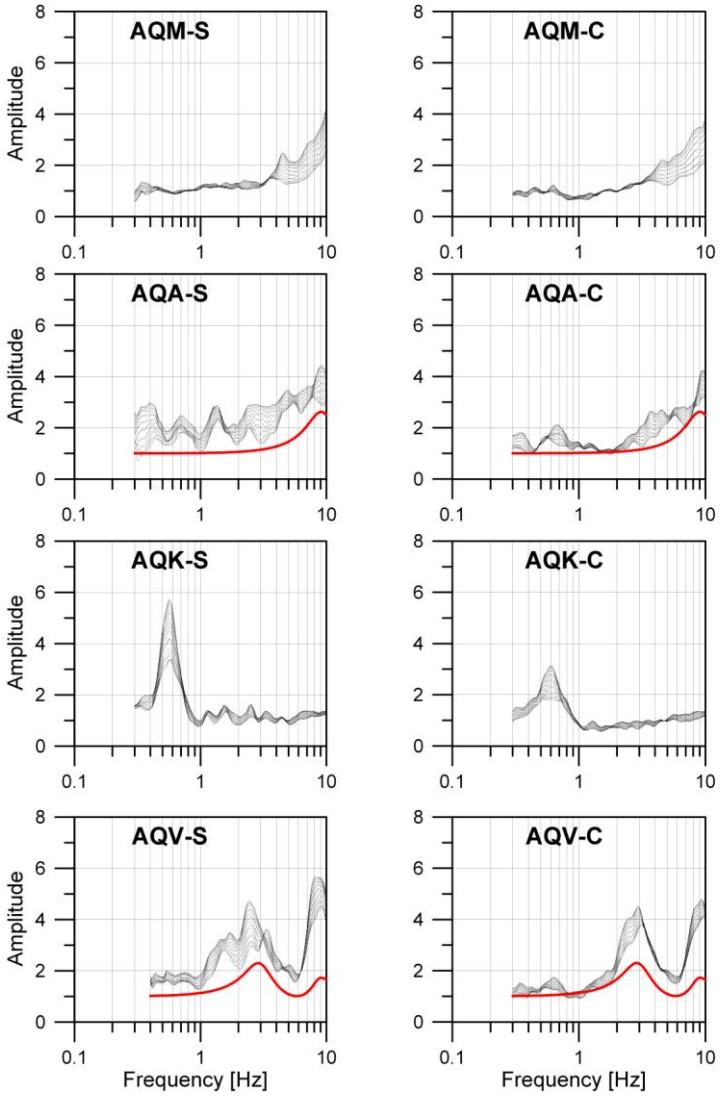

Fig. 3. Directional HVSR for the stations AQA, AQM, AQK and AQV (left panels show the S-wave phase, right panels the signal coda). The red line indicates the 1D linear soil response.

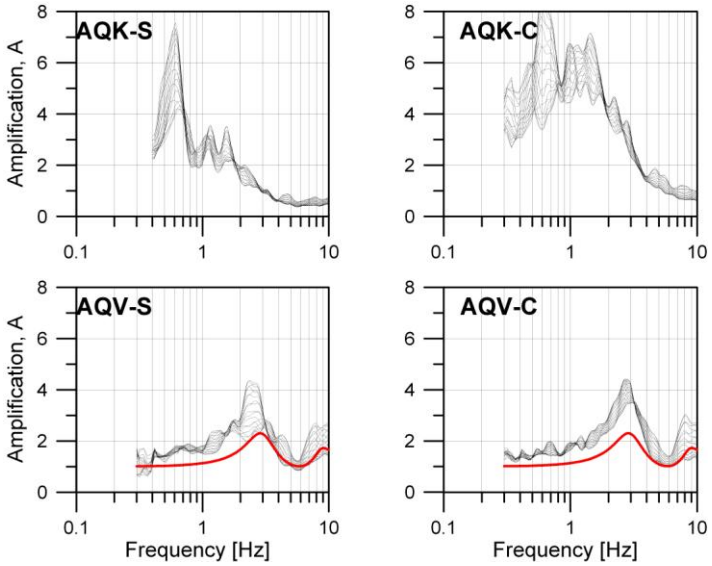

Fig. 4. Directional SSR for the stations AQA, AQK and AQV with AQM as reference. The red line indicates the 1D linear soil response.

The 1D response curves of a shear wave vertically propagating through the horizontal layers, with the profiles reported in Figure 2, are superimposed on the empirical curves of stations AQA and AQV. We could not evaluate the 1D response at AQK, as the available velocity profile has not reached the bedrock.
The 1D response curve of sites AQA and AQV is consistent with the empirical response in terms of fundamental frequency, f_0, both for S- and coda-waves analyses. At AQV station, the theoretical amplification underestimates the amplitudes detected by SSR analysis. This discrepancy is due to the low impedance contrast between bedrock and soil, set in the 1D model, as a probable consequence of the low S-wave velocity sampled in the fractured limestone at depth of 50m (Working Group ITACA, 2009).

Results at AQV station

We selected station AQV to investigate the presence of non-linear effects in the strong motion data. We increased the dataset used for the spectral analysis adding about 60 events with local magnitude between 3.0 and 3.5 (INGV-DPC S5 project, 2005-2007, http://dpc-s5.rm.ingv.it/). Table 2 reports only the strong-motion parameters estimated at AQM and AQV for the strongest events used in the analyses. The SSR computed on the S-phase and the coda waves (Figure 5) indicates that the amplification at AQV is maximized along a direction between 20 and 40 degrees (from the North), which corresponds to the direction perpendicular

to the major axis of the valley. All the subsequent spectral analyses are therefore carried out on the horizontal components projected along 30° direction.

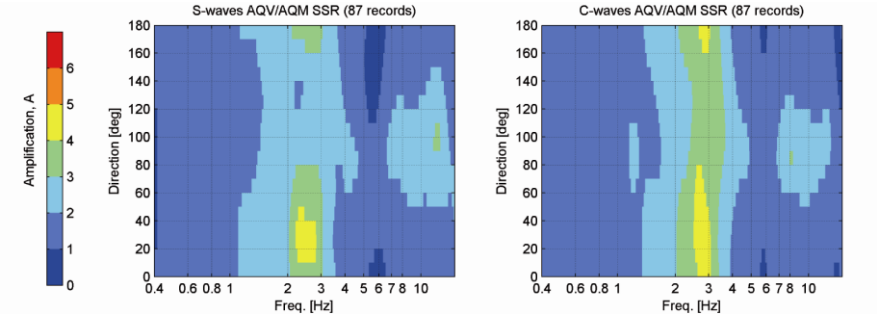

Fig. 5. Directional SSR (left: S-wave phase; right: coda waves)

Table 2. Peak ground motion parameters of the strongest events occurred in the epicentral area recorded by AQV and AQM. Data used in the SSR analysis are indicated in italic. The main-shock, recorded only by AQV station, is reported in bold. Peak Ground Acceleration (PGA), Significant Duration (D_S), Housner Intensity (I_H) and Arias Intensity (I_A) are referred to the maximum between the NS and the EW components. D_S is the time interval between 5% and 95% of the normalized Arias Intensity (Trifunac and Brady, 1975), while I_H is evaluated in the range 0.1 - 2.5 seconds (Housner, 1965).

			AQV					AQM				
Event time [yyyy-mm-dd hh:mm:ss]	M_W	M_L	PGA [cm/s^2]	D_S [s]	I_H [cm]	I_A [cm/s]	R_{EPI} [Km]	PGA [cm/s^2]	D_S [s]	I_H [cm]	I_A [cm/s]	R_{EPI} [Km]
2009-03-30 13:38:39		*4.1*	*141*	*2.6*	*2.9*	*2.6*	*6.8*	*44*	*4.4*	*1.7*	*0.6*	*6.8*
2009-04-06 01:32:39	**6.3**	**5.8**	**644**	**7.7**	**131.6**	**282.5**	**4.9**					
2009-04-06 02:37:04	5.1	4.6						332	3.2	12.8	18.4	1.6
2009-04-06 16:38:09	*4.4*	*4.0*	*74*	*3.5*	*3.2*	*2.4*	*1.9*	*80*	*2.5*	*3.2*	*3.3*	*2.3*
2009-04-06 23:15:37	5.1	4.8	148	4.5	10.3	5.8	8.4					
2009-04-07 09:26:28	*5.0*	*4.7*	*184*	*3.7*	*5.9*	*9.8*	*3.9*	*55*	*3.9*	*3.4*	*2.3*	*4.2*
2009-04-07 17:47:37	*5.6*	*5.3*	*144*	*5.4*	*14.8*	*13.0*	*15.1*	*124*	*5.0*	*8.3*	*5.2*	*14.9*
2009-04-07 21:34:29	*4.6*	*4.2*	*339*	*1.2*	*13.8*	*22.3*	*2.7*	*232*	*2.2*	*9.0*	*10.8*	*2.2*
2009-04-09 00:52:59	*5.4*	*5.1*	*152*	*5.5*	*17.3*	*9.8*	*11.9*	*86*	*5.9*	*9.4*	*3.1*	*11.7*
2009-04-09 19:38:16	5.3	4.9	100	5.5	5.7	3.6	13.8					
2009-04-13 21:14:24	*5.1*	*4.9*	*59*	*5.5*	*4.8*	*1.8*	*14.2*	*50*	*4.2*	*3.1*	*1.3*	*14.0*

Temporal variation of SSRs and HVSRs

In order to detect long time variation of the fundamental frequency f_0 for the AQV site, we estimate the fundamental frequency from the SRRs of recordings spanning from 15 hours to 21 days after the mainshock occurrence and average them on log-spaced intervals (Figure 6). No clear trend in the f_0 variation is observed. It can just be noted that f_0 slightly increases with time, from 2.4 Hz within the first week after the mainshock to 2.8 Hz in the following days. The coda analysis gives larger f_0 values with respect to the S-phase (Figure 6a), that are constant over time. On the other hand, the f_0 estimated from AQV waveforms with PGA larger than 80 cm/s^2 (except of the event of April 9) have lower f_0 values, in the range 1.9 - 2.1 Hz (blue points in Figure 6b). This result suggests that non linear effects at AQV can be associated to the amplitude and duration of the S-wave propagation through the soil underlying the station, although it has to be taken into account that frequency variation never exceeds the half width of the peak at mid-amplitude, plotted as error bars in Figure 6.

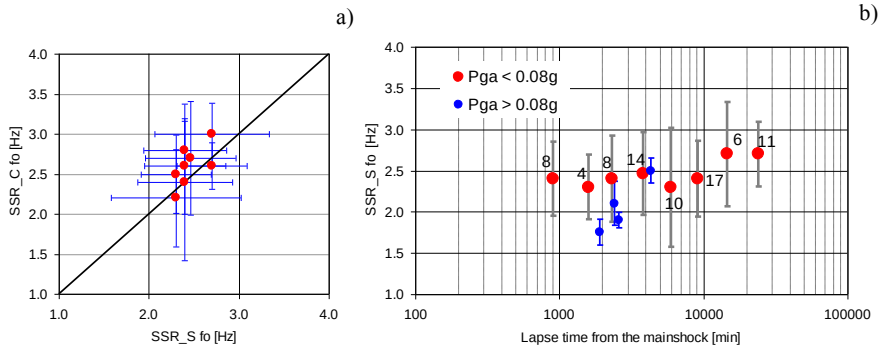

Fig. 6. a) Average fundamental frequency (f_0) from S_wave window versus average fundamental frequency from coda window. The vertical and horizontal bars indicate the standard deviation. b) Average fundamental frequencies from S wave window (red) versus time. Numbers indicate averaged f_0 for each time interval. Blue points are the f_0 estimated by AQV records having PGA larger than 80 cm/s^2. The half width of the peak at mid-amplitude is plotted as error bar.

SSR and HVSR versus PGA

Figure 7 (top panels) shows the SSRs calculated at AQV. The records have been grouped according to the PGA value, using a threshold of 80 cm/s^2. The SSR computed using the S-wave phase indicate a f_0 centered at about a 2Hz for the stronger events, while the frequency is about 3 Hz in case of weak events, very similar to the frequency obtained with the 1D linear model (see Figure 4). When the SSR is computed on the coda waves, there is no difference in the f_0 evaluated

either from strong or weak events. This leads us to hypothesize that whether there is a loss of soil stiffness it should occur during the S-wave phase. The same difference between the spectral ratios calculated on the S-wave phase and coda waves could be observed for the HVSRs (bottom panels of Figure 7). The mean curve obtained with the records with PGA < 80 cm/s^2 has two peaks, the first at about 1.6 Hz and the second at about 2.5 Hz. Moreover, to compute the HVSR we could use the mainshock record, which indicates a fundamental frequency lowering observed in the S-wave as well as in the coda.

In order to show the reduction of soil stiffness occurring during the S-wave phase, we calculated the SSR in function of time during the strongest aftershocks recorded simultaneously at AQV and AQM (see Table 2). We present only the results relevant to the Mw 5.0 event occurred on 2009-04-07 at 09:26:28 GMT (Figure 8), although the PGA recorded at AQV for this event is 184 gal, lower than the 339 gal associated to the Mw 4.6 event occurred on 2009-04-07 21:34:29 GMT. The latter is, in fact, an impulsive event with large PGA and very short effective duration (1.2s; see table 2).

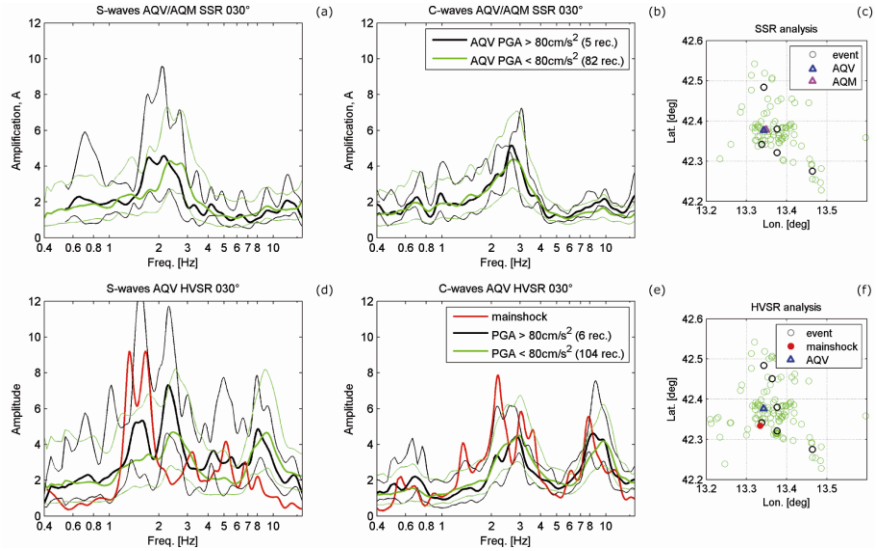

Fig. 7. SSRs and HVSRs for strong (PGA > 80 gal) and weak events (PGA < 80 gal) for station AQV, projected along 30°N: SSR computed on S-phase (a) and on coda waves (b); HVSR computed on S-phase (d) and on coda waves (e). The HVSR relative to the mainshock is plotted in red. Maps (c) and (f) show the epicentre of the analyzed events and AQV and AQM location. Black and green circles indicate strong and weak events, respectively.

We set a local origin at the S wave arrival time, in order to avoid the contamination of P and S phases, and we calculated the Fourier spectra for moving windows having length of 1.67s, with no overlap. In the first 3 seconds after the S-wave arrival, corresponding to the release of the most energetic part of the signal, the fundamental frequency assumes a value lower than 2 Hz. The frequency gradually in-

creases afterwards, reaching a value of 3 Hz at 6 s. The mainshock was only recorded by station AQV, therefore we can only calculate the variation of HVSR with time, using the same procedure adopted for the time dependent SSR. The fundamental frequency of the site is lower than 2Hz for the first 10s after the S-phase arrival, then the frequency increases and stabilizes at 3Hz, the characteristic value of this site at low deformation (Figure 9).

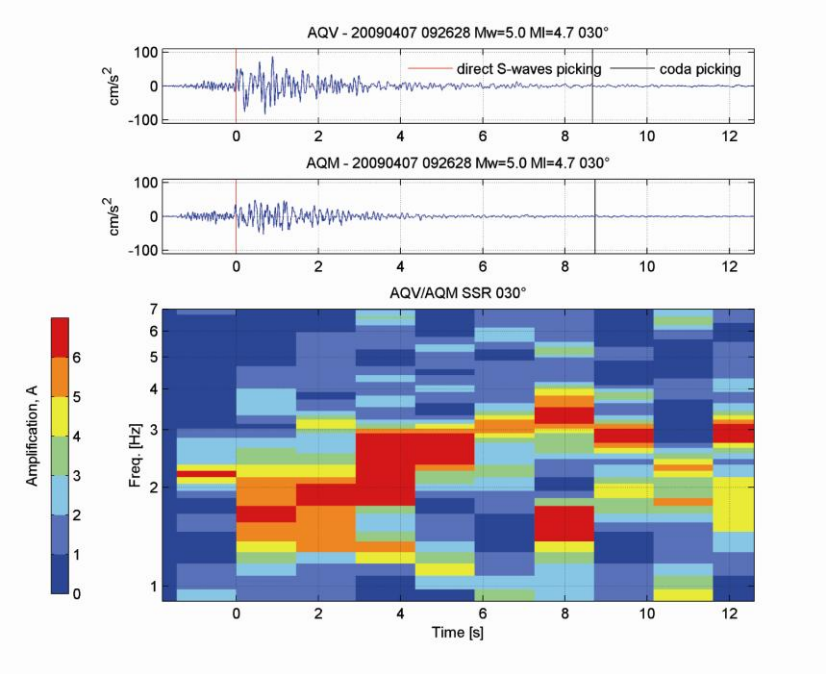

Fig. 8. Time dependent SSR for the 2009-04-07 09:26:28 aftershock.

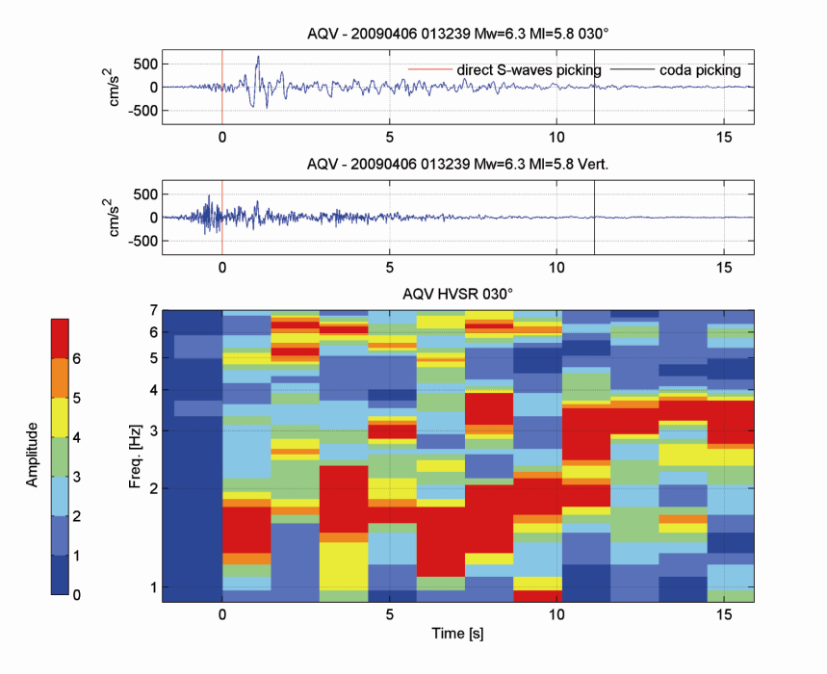

Fig. 9. Time dependent HVSR for the mainshock.

1D linear-equivalent modeling

In order to verify the reduction of the soil fundamental frequency, we modeled the 1D equivalent linear soil response of AQV using the SHAKE-91 software (Idriss and Sun, 1992). The soil profile used in modeling is reported in Figure 2, and the variation of the shear modulus and the equivalent damping ratio with shear strain for gravels is evaluated by adopting two different models, proposed by Rollins et al. (1998) and Seed et al. (1986). As the mainshock and some of the largest aftershocks of the sequence were not recorded by the bedrock station AQM, we calculated the rock outcrop waveforms from the AQV records. The results were compared with the corresponding records at AQM, both in time and frequency domain (in terms of response spectra), to verify the degree similarity of the synthetic and observed records. Figure 10 shows the results for the 2009-04-07 09:26:28 aftershock. The comparison is satisfactory, mainly in the frequency range in which the site AQV amplifies (about 3 Hz).

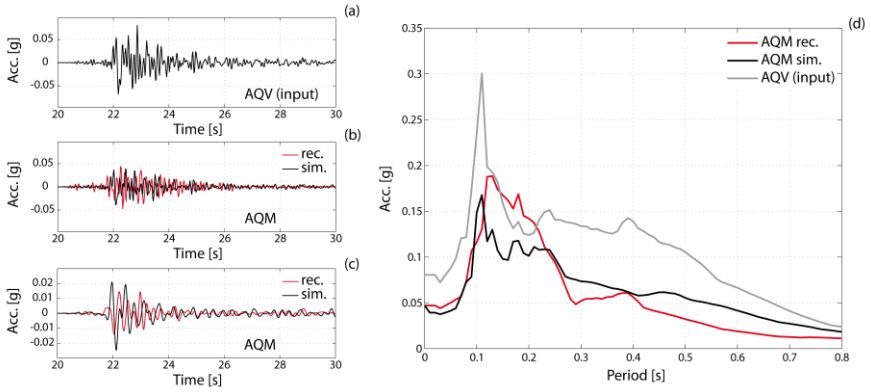

Fig. 10. 1D simulation of the 2009-04-07 09:26:28 aftershock: (a) seismic input; b) comparison between synthetic and unfiltered record at AQM; (c) comparison between synthetic and band-pass filtered (4^{th} order Butterworth) record at AQM, in the range 1-4.5 Hz; (d) 5% damped response spectra obtained from the acceleration time histories displayed in (a) and (b).

In Figure 11a, the 1D equivalent-linear amplification function (mean ± 1 standard deviation) simulated for the five strongest aftershocks are compared with the average SSRs obtained analyzing the S phase windows of the same events. The used soil curves are from Rollins (1998). The fundamental frequency during the strongest aftershocks does not decrease and is rather similar to the frequency evaluated from the empirical SSR curves. If the curves from Seed *et al*. (1986) are used for the simulation there is an evident decrease of the fundamental frequency (Figure 11b). The modeling of the mainshock produces a lowering of the f_0, more pronounced when the Seed *et al*. (1986) curves are assumed (Figure 11b and 11d).
The simulations demonstrate that the results are strongly dependent on the assumed variation of the shear modulus and damping ratio with strain. The curves by Seed et al. (1986) better reproduce the frequency shift occurred during the mainshock and the largest aftershocks. The 1D model only allows verifying the reduction of the soil stiffness with strain, compatible with the decrease in the fundamental frequency.

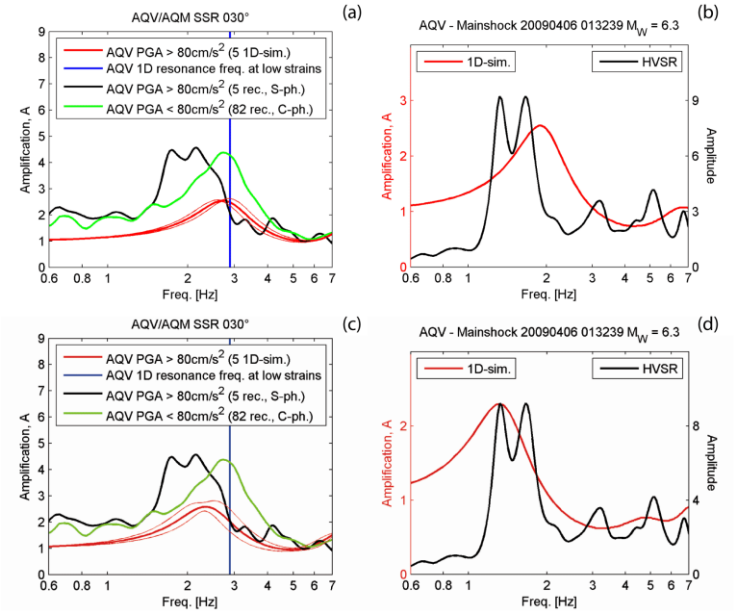

Fig. 11. 1D simulations: a) 1D response relative to the strongest aftershocks (red lines represent the average ± 1standard deviation of the simulations assuming the Rollins (1998) soil curves) compared to the relevant SSR; b) 1D response curve of the mainshock (red line) assuming the Rollins (1998) soil curves and HVSR obtained from the analysis of the mainshock record at AQV. c) d) same as a) and b) assuming the Seed et al. (1986) soil curves.

Short scale variation using S-Transform analysis

This section will focus on intra-event soil behavior, using single events. Different techniques are proposed in the literature, such as the Short Time Fourier Transform (STFT), the Wavelet Transform (WT) or, as in this study, the Stockwell Transform (S-Transform). The latter is particularly useful to analyse the time-frequency behavior of a system that changes its dynamic characteristics during time. In fact, it provides information about the local spectrum of a generic signal (Stockwell et al., 1996) overcoming the limitations derived from the assumptions of the stationarity of a signal. This transformation, for a signal *h(t)*, is defined as:

$$S(\tau, f) = \frac{|f|}{2\pi} \int_{-\infty}^{+\infty} h(t) \cdot e^{-\frac{(\tau - t)^2 \cdot f^2}{2}} \cdot e^{-i \cdot 2 \cdot \pi \cdot f \cdot t} dt \qquad (2)$$

where t is time, f is frequency and τ is a parameter that controls the position of the Gaussian window along the time axis. Examples of application of S-transform on nonlinear dynamic behavior of soil and buildings can be found in Ditommaso *et al.* (2010).

In this section we show the results obtained from the analyses of the ground motion recorded by stations AQA, AQG, AQK, AQM, AQV, MI01, MI02, MI03 and MI05. Although several aftershocks were recorded by these stations, only one event is considered in this section in order to synthesize the results. According to the spectral analyses shown in the previous sections, we rotated the accelerometric time series in the horizontal plane to obtain the maximum PGA value and the maximum Housner Intensity (Housner, 1952) I_H value for each trace. It is worth to note that the maximum PGA and I_H are not found along the same horizontal direction.

The main information about the selected events is reported in Table 3. In order to synthesize the results, we report only the parameters recorded along the direction for which the I_H is maximum, being I_H a parameter better correlated to the energy content of an earthquake rather than PGA to analyze the response of soils and buildings (see e.g., Masi *et al.*, 2010). It is worth noting that while the maximum PGA value was recorded at AQV during the mainshock, the M=5.6 aftershock recorded at MI05 has a PGA larger than the mainshock at the remaining RAN stations.

Table 3. Characteristics of the selected events.

				PGA		I_H	
Station Code	Date	Time	M_W	Azimuth [deg]	MAX [g]	Azimuth [deg]	MAX [m]
AQA	06/04/2009	01:32:39	6.3	160	0.446	130	0.867
AQG	06/04/2009	01:32:39	6.3	170	0.490	150	1.068
AQK	06/04/2009	01:32:39	6.3	150	0.387	140	1.478
AQM	07/04/2009	17:47:37	5.6	10	0.127	90	0.094
AQV	06/04/2009	01:32:39	6.3	120	0.770	80	1.162
MI01	07/04/2009	17:47:37	5.6	80	0.235	70	0.163
MI02	07/04/2009	17:47:37	5.6	20	0.217	170	0.238
MI03	07/04/2009	17:47:37	5.6	100	0.133	80	0.259
MI05	07/04/2009	17:47:37	5.6	70	0.698	60	0.618

At each station, ambient noise was also recorded by mean a three-directional tromometer, in order to compare the stationary and the non stationary response to detect a possible nonlinear behavior of the soil. If the soil behavior is stationary and linear, the fundamental frequency should be constant over time. Moreover, in order to check possible variations of stationarity, we focus on the energy variation over time in a neighborhood of the fundamental frequency. In order to obtain a synthetic representation of the results for each station, one figure includes infor-

mation derived from accelerometric and noise recordings. Each figure shows the accelerometric recording on top-left, the S-Transform on left-bottom and the HVSR on the right-bottom panel. The same frequency scale is used for both the S-Transform and the HVSR, to verify whether the fundamental frequency obtained from the noise recording, remains constant during the S-waves phase until the co-da-waves to the end of the signal.

Analysis of the non-stationary site response

In this paragraph we report the observation for the recordings that show a non-stationary behavior. Using the standard defined above, Figure 12 reports the results of the analyses for the AQK site. Using ambient vibration measurements the fundamental frequency estimated for the soil is 0.62±0.01 Hz, where 0.01 Hz is the uncertainty related to the sampling frequency and the time-window length adopted for the analysis. For the AQK site there is a slight change of fundamental frequency over time during the mainshock. In particular, at the beginning of the signal the f_0 is 0.65±0.01 Hz, while the minimum frequency value becomes 0.57±0.01 Hz at 12.12s. At the end of the record the fundamental frequency returns to the starting value. It is worth to note that the minimum frequency is not occurring when the time series reaches the maximum acceleration.
For the AQK case two figures are reported: Figure 12a shows the standard S-Transform, while Figure 12b reports the S-Transform normalized to the maximum of each time step. The normalized S-Transform allows to better identifying the site fundamental frequency, while the standard S-Transform is more useful to identify the instant-by-instant frequency content of the signal, its change over time and the related energy.

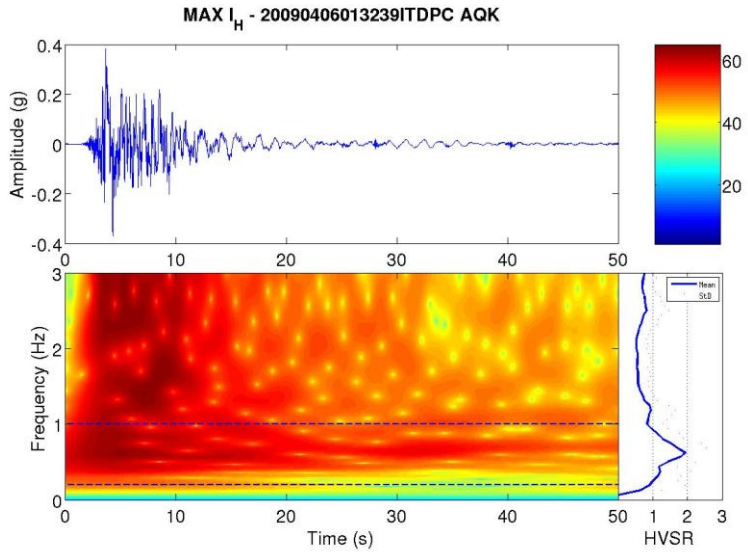

(a)

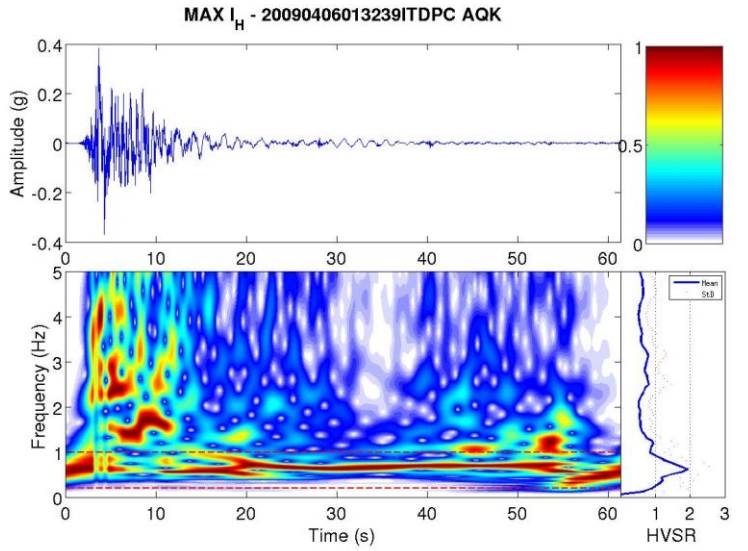

(b)

Fig. 12. L'Aquila mainshock recorded at AQK station: a) bottom left: S-Transform; bottom right: HVSR curve; b) bottom left: normalized S-Transform and same features as in a).

The fundamental frequency estimated for the AQV site is equal to 3Hz (cf. AQV monography on http://itaca.mi.ingv.it). The noise HVSR does not allow identifying a clear peak but instead a plateau that ranges 2.5 to 3.5Hz.

The accelerometric recording exhibits a non stationary behavior in the frequency range of interest (see Figure 13). The fundamental frequency has a starting value of 2.52±0.02 Hz , then reaches a minimum equal to 2±0.02Hz at 10.24s and afterwards comes back to the starting value. The frequency change over time observed at the AQV station, seem to produce temporary changes in the dynamic properties of the site, on a short time scale.

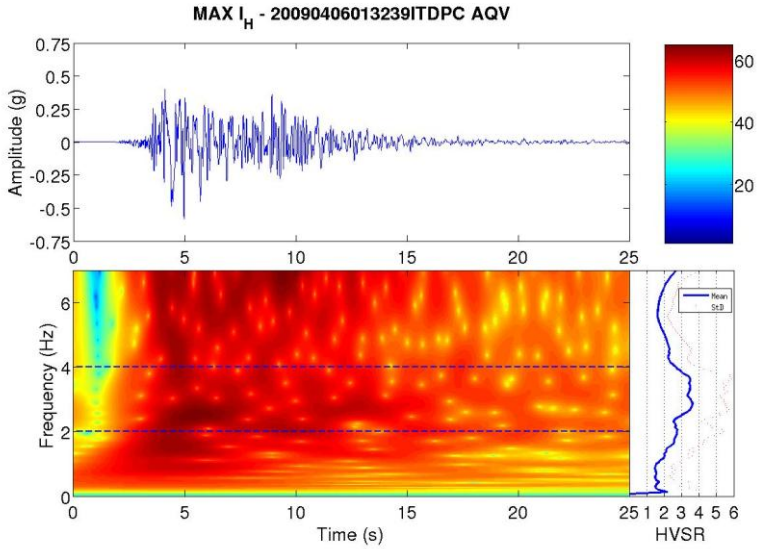

Fig. 13. L'Aquila mainshock recorded at AQV station. Bottom left: time-frequency; bottom right: HVSR curve.

The temporary stations recorded only the main aftershocks. Station MI03 (Figure 14) shows minor differences when comparing the results obtained from the accelerometric and noise recordings. The fundamental frequency estimated from ambient noise is equal to 3±0.02Hz, during the strong motion phase there are minor changes and the final value is the same as at the start. It is interesting to note that the fundamental frequency decreases (see arrow in Figure 14) at about 3 s, when the energy of the signal is not the maximum, while it can be seen a slight frequency increase around 5 s when PGA occurs.

The last examined temporary station is MI05. From the ambient noise the estimated fundamental frequency is equal to 3±0.01Hz (Figure 15). The time-frequency analysis depicts a non-stationary soil behavior, as during the earthquake the minimum value of the fundamental frequency is equal to 2.7±0.03Hz.

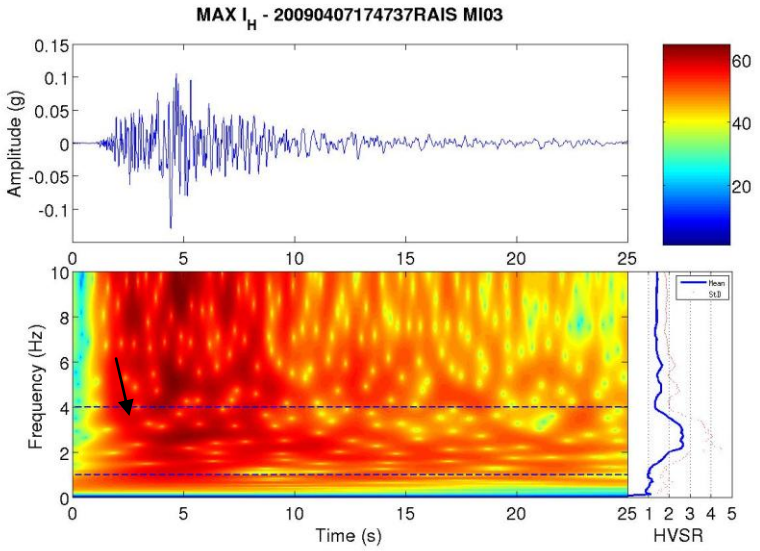

Fig. 14. L'Aquila aftershock (07/04/2009 17:47) recorded at MI03. Bottom left: time-frequency; bottom right: HVSR curve.

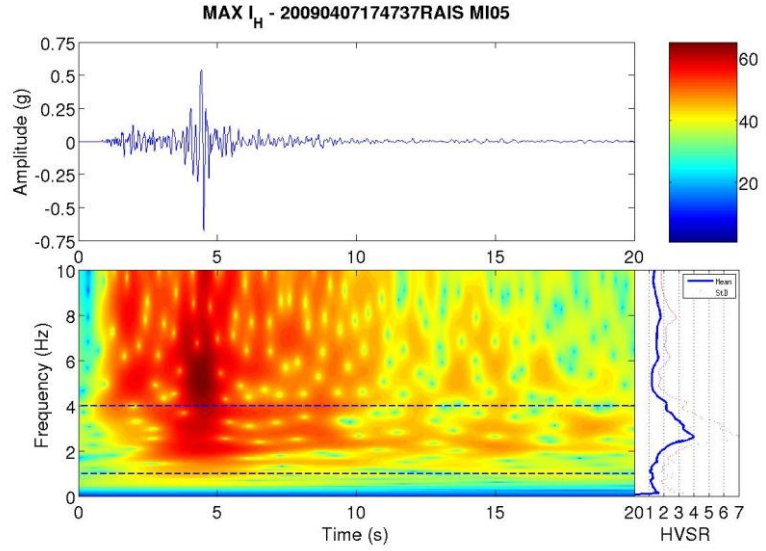

Fig. 15. L'Aquila aftershock (07/04/2009 17:47) recorded at MI05. Bottom left: time-frequency; bottom right: HVSR curve.

In this sub-paragraph we will examine the stations that showed a stationary response. In the following figures the represented frequency range is 0-10Hz, and we adopted again a logarithmic scale for the S-Transform amplitude.
The accelerometric recording of the AQA station (Figure 16) do not show a clear time-varying dynamic behavior of the soil. In fact, the fundamental frequency estimated for the soil (9±0.01Hz) does not change over time, and energy appears scattered on a wide band rather that concentrated on restricted frequencies.

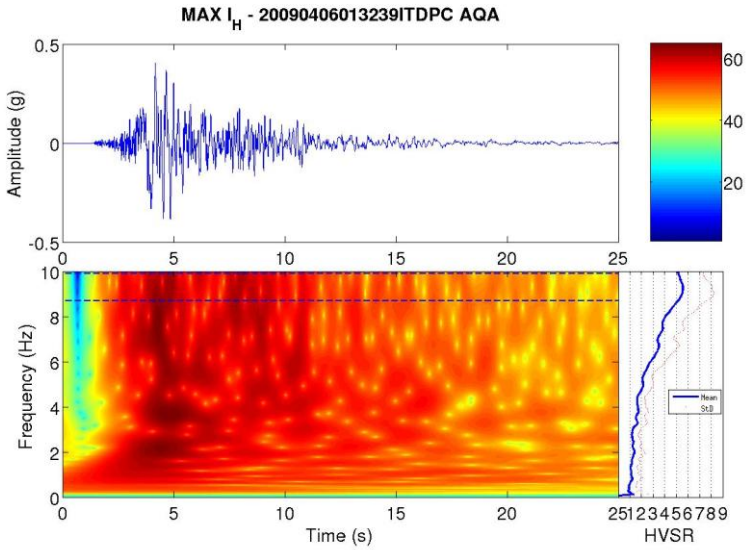

Fig. 16. L'Aquila mainshock recorded at AQA station. Bottom left: time-frequency analysis; bottom right: HVSR curve.

In Figure 17 the results for AQG station are reported. From ambient vibration measurements the estimated fundamental frequency of the soil is 5±0.01Hz and it is clear from the time-frequency analysis that in frequency range 4-6 Hz the accelerometric signal exhibits a stationary behavior.
Figure 18 show the results of the analysis on the accelerometric and noise recordings relative to the AQM site. The fundamental frequency estimated from the noise measurements is about 8Hz, although a clear peak is not identifiable. On the contrary, there is a ramp starting at 4Hz, with amplitude equal to 3 that reaches a maximum value of 4 at 8Hz. However, from the S-Transform it is clear that in the examined frequency range (7-9Hz) the accelerometric signal does not show a time-varying behavior.
Results of the analysis on the MI01 station are shown in Figure 19. There is a clear peak at the fundamental frequency equal to 6±0.02Hz. From the S-Transform in the frequency range of interest the signal does not evidence a nonlinear behavior of the soil.

In Figure 20 the results obtained for the MI02 station are depicted. From ambient noise the estimated fundamental frequency is equal to 5±0.02Hz and from the S-Transform the soil behavior also appears stationary over time.

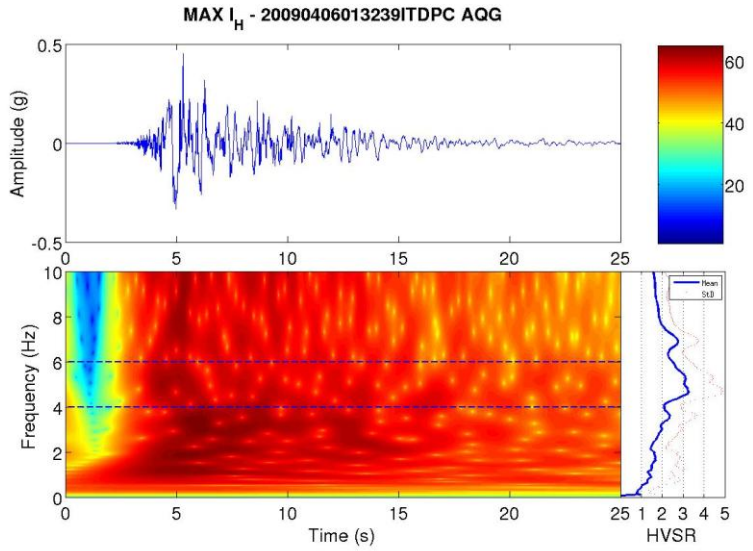

Fig. 17. L'Aquila mainshock recorded at AQG station. Bottom left: time-frequency analysis; bottom right: HVSR curve.

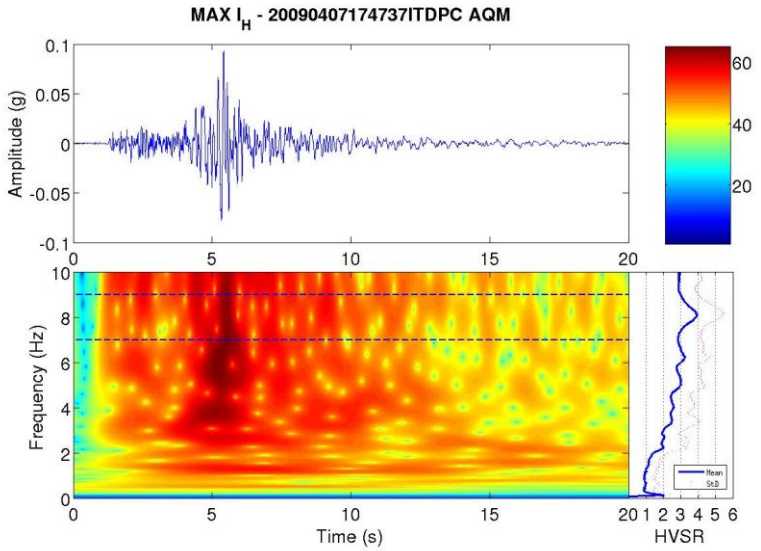

Fig. 18. L'Aquila mainshock recorded at AQM station. Bottom left: time-frequency analysis; bottom right: HVSR curve.

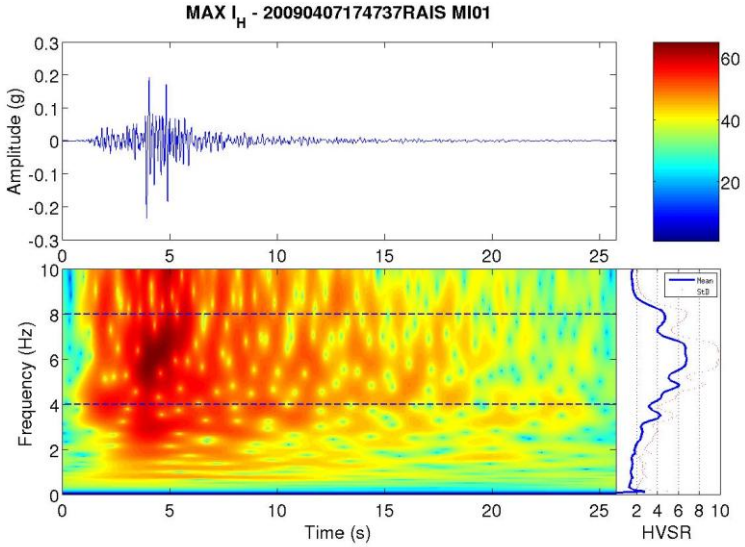

Fig. 19. L'Aquila aftershock (07/04/2009 17:47) recorded at MI01 station. Bottom left: time-frequency analysis; bottom right: HVSR curve.

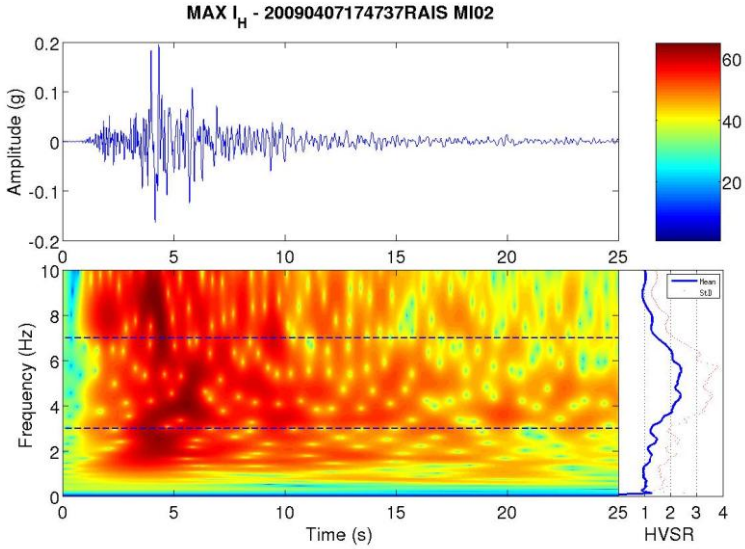

Fig. 20. L'Aquila aftershock (07/04/2009 17:47) recorded at MI02 station. Bottom left: time-frequency analysis; bottom right: HVSR curve.

Discussion and conclusion

Past literature showed long and short time variation of site amplification and soil fundamental frequency, attributing these phenomena to non-linear soil behavior. It was assumed an inelastic, softening non-linearity, since the original frequency and amplification were both decreasing and not recovering for a time varying from few hours to several months. During the L'Aquila, 2009 seismic sequence it was possible for the first time to test these hypothesis in Italy, because of the strongest accelerations ever recorded (PGA on a single rotated component exceeding 0.7 g) and the availability of data in the fore-, main- and after-shock phase recorded by permanent and temporary networks.
Concerning the long time scale, little variation was observed at the permanent stations of the Aterno Valley array. The only clear evidence was a slight decrease of the fundamental frequency in the days immediately following the mainshock at AQV site, which mainly occurred in correspondence of the S- phase arrivals during the strongest aftershocks.
As for the short time-scale variation, the evidence was often contrasting, with some station showing a time-varying behavior while others did not change their frequency with respect to the one measured using noise HVSR. Even when a time-varying fundamental frequency was observed, it was difficult to attribute it to a classical, softening non-linear behavior due to the following reasons:

1. sometime the frequency increases instead of decreasing;
2. the minimum of frequency is not correlated to the maximum amplitude of acceleration recordings;
3. at the end of the recordings the original frequency is always recovered, i.e. there is not a long lasting modification of the soil stiffness.

Possible explanations of the observed variations are:

1. Frequency variation with time is not directly related to soil stiffness, but to peculiar phases of the seismic signal whose frequency is more related to source effect (the sites are located in the near source) such as directivity and flings (as proposed for this quake by Chioccarelli and Iervolino 2010). However this phenomena is not observed at all stations, although they are very close each other with respect to the epicenters.
2. The Aterno Array stations are located on sites where coarse, cohesionless materials prevail over fine-grained cohesive ones. The River Aterno causes the water table to be very close to the surface, thus providing the conditions where poroelasticity may play a role causing non-linear behavior (Bonilla *et al*., 2005) that can be quickly reversed if the permeability is large enough to dissipate the build up of fluid pressure associated to the strong motion phase. Unfortunately, no real-time piezometers are available in the area to support this hypothesis.

These results suggest that caution should be taken in performing site specific hazard estimate that take into account the local seismic response modeled by simple 1-D, vertically propagating waves in strongly non-linear material.
Even for the strongest shocks recorded during L'Aquila sequence, variations in frequency and amplitude seem not very important from building design standpoint. The only exception seems to be the site named AQV, where the analyses evidences a fundamental frequency of the soil which changes during the mainshock from 3 Hz to about 1.5 Hz.

References

Bindi, D., Pacor, F., Luzi, L., Massa, M., Ameri, G.: The Mw 6.3, 2009 L'Aquila earthquake: source, path and site effects from spectral analysis of strong motion data. Geophysical Journal International, 179, 3, 1573-1579 (2009)

Bonilla., L.F., Archuleta, R.J., Lavallée, D.: Histeretic and dilatant behavior of cohesionless soils and their effects on non-linear site response: field data observation and modelling. Bull. Seism. Soc. Am., 95, 2373-2395 (2005)

Chioccarelli, E., Iervolino, I.: Near Source seismic demand and pulse-like record: A discussion for L'Aquila earthquake. Earthquake Engineering and Structural Dynamics, 39, 1039-1062 (2010)

De Luca, G., Marcucci, S., Milana, G., Sanò, T.: Evidence of low frequency amplification in the city of L'Aquila, Central Italy, through a multidisciplinary approach including strong- and weak-motion data, ambient noise, and numerical modeling. Bull. seism. Soc. Am., 95, 1469–1481 (2005). doi:10.1785/0120030253.

De Martin, F., Kawase, H., Modaressi-Farahmand Razavi, A.: Nonlinear Soil Response of a Borehole Station Based on One-Dimensional Inversion during the 2005 Fukuoka Prefecture Western Offshore Earthquake. Bulletin of the Seismological Society of America, Vol. 100, No. 1, pp. 151–171 (2010)

Ditommaso, R., Mucciarelli, M., Ponzo, F.C.: S-Transform based filter applied to the analysis of non-linear dynamic behaviour of soil and buildings. 14th European Conference on Earthquake Engineering. Proceedings Volume. Ohrid, Republic of Macedonia. August 30 - September 3 (2010).

Gorini, A., Nicoletti, M., Marsan, P., Bianconi, R., De Nardis, R., Filippi, L., Marcucci, S., Palma, F., Zambonelli, E.: The Italian strong motion network. Bulletin of Earthquake Engineering. Volume 8, Number 5, 1075-1090 (2010)

Herraiz, M., Espinosa, A.F.: Coda waves: A review. Pure and Applied Geophysics, vol. 125, n. 4, 499-577 (1986). doi: 10.1007/BF00879572

Housner, G.: Spectrum intensities of strong motion earthquakes. Proceedings Symposium on Earthquake and Blast Effects on Structures, Los Angeles, California, 20-36 (1952)

Konno, K., Ohmachi, T.: Ground-motion characteristic estimated from spectral ratio between horizontal and vertical components of microtremor, Bull Seism Soc Am, 88, 228-241 (1998)

Idriss, I.M., Sun, J.I.: User's Manual for SHAKE91. Center for Geotechnical Modeling, Department of Civil Engineering, University of California, Davis. http://nisee.berkeley.edu-/elibrary/Software/SHAKE91ZIP (1992). Accessed 26 June 2007.

Masi, A., Chiauzzi, L., Braga, F., Mucciarelli, M., Vona, M., Ditommaso, R.: Peak and integral seismic parameters of L'Aquila 2009 ground motions: observed versus code provision values. Bull Earthquake Eng (2010). doi: 10.1007/s10518-010-9227-1

Massa, M., Pacor, F., Luzi, L., Bindi, D., Milana, G., Sabetta, F., Gorini, A., Marcucci S.: The ITalian ACcelerometric Archive (ITACA): processing of strong-motion data. Bull Earthquake Eng, 8, 5, 1175-1187 (2010). doi: 10.1007/s10518-009-9152-3

Mayeda, K., Malagnini, L., Walter, W.R.: A new spectral ratio method using narrow band coda envelopes: evidence for non-selfsimilarity in the Hector Mine sequence, Geophy. Res. Lett., 34, L11303, (2007). doi: 10.1029/2007GL030041

Rollins, K.M., Evans, M.D., Diehl, N.D., Daily III, W. D.: Shear Modulus and Damping Relationships for Gravels. J. Geotech. and Geoenvir. Engrg., 124, 5, 396-405 (1998)

Rubinstein, J. L., Uchida, N., Beroza, G.C.: Seismic velocity reductions caused by the 2003 Tokachi-Oki earthquake. J Geophys Res, 112, B05315 (2007). doi 10.1029/2006JB004440

Sawazaki, K., Sato, H., Nakahara, H., Nishimura, T.: Time-Lapse Changes of Seismic Velocity in the Shallow Ground Caused by Strong Ground Motion Shock of the 2000 Western-Tottori Earthquake, Japan, as Revealed from Coda Deconvolution Analysis, Bullettin of the Seismological Society of America, 99, 1, 352-366 (2009)

Sawazaki, K., Sato, H., Nakahara, H., Nishimura, T.: Temporal change in site response caused by earthquake strong motion as revealed from coda spectral ratio measurement, Geophys. Res. Lett., 33, L21303 (2006). doi:10.1029/2006GL027938.

Seed, H.B., Wong, R.T., Idriss, I.M., Tokimatsu, K.: Moduli and Damping Factors for Dynamic Analyses of Cohesionless Soils. J Geotech Engrg, 112, 11, 1016-1032 (1986)

Stockwell, R.G., Mansinha, L., Lowe, R.P.: Localization of the complex spectrum: the S transform. IEEE Trans. Signal Process., 44, 998-1001 (1996)

Trifunac, M.D., Brady, A.G.: A study on the duration of strong earthquake ground motion. Bull Seis Soc Am, 65, 581-626 (1975)

Wu, C., Peng, Z., Ben-Zion, Y.: Non-linearity and temporal changes of fault zone site response associated with strong ground motion. Geophys. J. Int., 176, 265–278 (2009). doi: 10.1111/j.1365-246X.2008.04005.x

Wu, C., Peng, Z., Assimaki, D.: Temporal Changes in Site Response Associated with the Strong Ground Motion of the 2004 Mw 6.6 Mid-Niigata Earthquake Sequences in Japan, Bull Seis Soc Am, 99, 6, 3487-3495 (2009)

Zambonelli, E., de Nardis, R., Filippi, L., Nicoletti, M., Dolce, M.: Performance of the Italian strong motion network during the 2009, L'Aquila seismic sequence (central Italy). Bull Earthquake Eng (2010). DOI 10.1007/s10518-010-9218-2